ACS OMEGA

http://pubs.acs.org/journal/acsodf

Article

Short Ligand, Cysteine-Modified Warnericin RK Antimicrobial Peptides Favor Highly Sensitive Detection of *Legionella pneumophila*

M. Amirul Islam, Walid M. Hassen, Azam F. Tayabali, and Jan J. Dubowski*

Cite This: *ACS Omega* 2021, 6, 1299−1308

Read Online

ACCESS | Metrics & More | Article Recommendations | Supporting Information

ABSTRACT: Culture-based methods for the detection of *Legionella pneumophila* are prohibitively slow and frequently inadequate. The problem has been addressed with biosensing technology that employs a variety of ligands for the specific capture of bacteria. However, the limited success of the application of mammalian antibodies, aptamers, and nucleic acid-based probes for sensitive biosensing has generated growing interest in exploring alternative biosensing architectures, such as those based on antimicrobial peptides (AMP) that are known for their attractive therapeutic applications. We report on the successful employment of cysteine-modified warnericin RK AMP for the operation of a highly sensitive biosensor of *L. pneumophila* based on digital photocorrosion of GaAs/AlGaAs nanoheterostructures. The replacement of the relatively cumbersome procedure commonly applied for the attachment of antibodies to COOH-terminated mercaptohexadecanoic acid self-assembled monolayers has allowed for a significant reduction in the distance at which bacteria are immobilized above the biosensor surface. An important consequence of this approach is the attractive limit of detection of *L. pneumophila* estimated at 2×10^2 CFU/mL. The target bacteria were captured four times more efficiently than *P. fluorescens*, *B. subtilis*, and *E. coli*, which is highly promising for environmental monitoring.

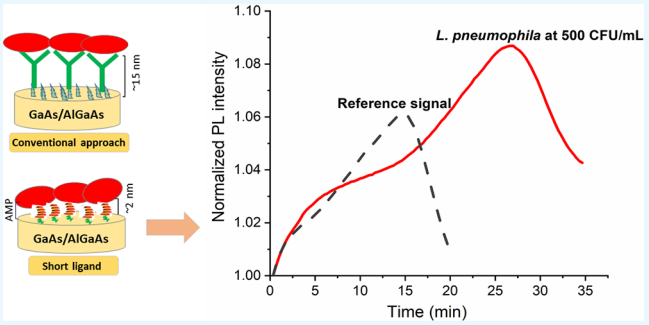

1. INTRODUCTION

Rapid detection of pathogenic bacteria in a water environment remains a challenging issue.[1,2] Of particular interest are rapid, portable, non-labor intensive, yet cost-attractive tools for detection of pathogens.[3] The culture-based, colony counting methods have been widely used to detect bacteria,[4] but they are labor and time intensive.[4,5] For instance, *Legionella pneumophila* may require up to 10 days of incubation for visible detection of colonies.[6] Alternatively, polymerase chain reaction (PCR)-based detection[7] or matrix-assisted laser desorption ionization time-of-flight (MALDI-TOF) spectroscopy[8] could both provide relatively fast and accurate detection. However, the need for highly trained personnel and sophisticated lab requirements are the main constraints of these techniques.[9,10] The biosensor-based detection methods of pathogenic bacteria have gained attention due to their potential to offer relatively fast, portable, and easy-to-handle solutions.[11] In that context, various types of *L. pneumophila* biosensors have been investigated ranging from optical[12,13] and piezoelectric[14,15] to electrochemical.[16,17] However, to the best of our knowledge, an economically attractive method for automated monitoring of water reservoirs for the presence of pathogenic bacteria has yet to be developed. Recently, photoluminescence (PL)-based detection of *E. coli* has proven to be rapid and relatively sensitive.[18] In this technique, the sensitivity of PL varies with the presence of electrically charged molecules (*i.e.*, proteins, viruses, and bacteria) on the surface of semiconductor nanoheterostructures that have the potential for the realization of a regenerable system designed for automated data collection.[19−22]

L. pneumophila is a pathogenic waterborne bacterium, predominantly found in man-made artificial water reservoirs, *i.e.*, spas and cooling towers.[23,24] Humans who are accidentally exposed may develop a pulmonary infection known as Legionnaire's disease.[24,25] In 2006, more than 6000 cases were reported in Europe, 400 of them are fatal.[25] Of the 60 reported *Legionella* species, 85−90% are associated with Legionnaire's disease.[26] Therefore, the detection of *L. pneumophila* in water reservoirs has emerged as a public health priority. Culture-based methods have been commonly applied for the detection of *L. pneumophila*;[27,28] however, they are inefficient. In addition to a multi-day delayed detection, some viable but non-culturable bacteria could not be detected with

Received: September 28, 2020
Accepted: December 14, 2020
Published: January 6, 2021

https://dx.doi.org/10.1021/acsomega.0c04753
ACS Omega 2021, 6, 1299−1308

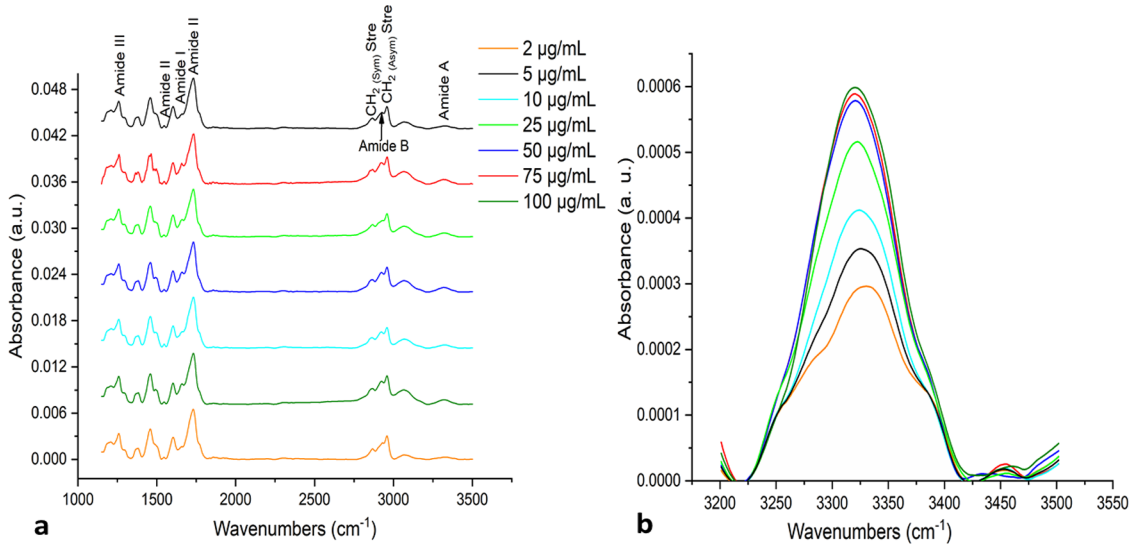

Figure 1. Representative FTIR absorbance spectra of thiol and peptide related peaks (a), and amide A absorbance spectra collected for different peptide concentrations (b).

these techniques. The PCR-based method can address most of the aforementioned problems, but the requirement of trained personnel and sophisticated laboratory facilities limit the application of this technique.[4] Biosensor-based detection of *L. pneumophila* has the potential to alleviate these deficiencies.

The efficiency of bio-recognition elements is crucial in order that biosensor technology be able to offer a selective, sensitive, and accurate measurement of the target.[29,30] Numerous bio-recognition elements, such as antibodies (Ab), carbohydrates, aptamers, peptides, as well as combinations of these, have been widely explored in different biosensing platforms.[11] Among them, Ab have been considered as an attractive option since they can be highly specific toward the antigenic target.[31,32] However, Ab suffer from lack of stability, especially under extreme environmental conditions, such as high/low pH and elevated temperatures,[31] and they often require additional conjugating compounds, such as neutravidin, biotin, or avidin.[33] These conjugations increase the number of interfaces, which could affect the reproducible performance of a biosensor. Recently, some studies have shown that antimicrobial peptides (AMPs) could be reasonable candidates for bio-recognition in biosensing platforms.[32,34,35] The multiple molecular niches of an AMP seem partially responsible for the strong interaction with bacteria and fungi surface moieties.[31] Furthermore, it has been reported that some cationic AMPs could maintain their activity in harsh environments, even after boiling and autoclaving.[36,37] The considerably superior stabilities of AMPs over those of typical globular proteins[31,37] justify the AMP research expected to lead to the replacement of typical Ab-based bio-recognition elements.

In the past few years, several AMPs such as magainin I,[38] clavanin A,[39] and polymyxin B[40] have been investigated as bio-recognition probes, with some AMPs demonstrating a highly specific recognition capacity.[31] Mannoor et al. reported that a gold electrode functionalized with magainin I AMP showed differential binding affinity to the pathogenic bacterial strains of *E. coli* and *Salmonella* at 10^7 CFU/mL.[31] Another study reported that a gold microelectrode functionalized with Leucocin A (Leu A) exhibited high binding affinity to *Listeria monocytogenes*.[41] It has been reported that warnericin RK is a membrane active peptide, which shows high specificity to *L. pneumophila*.[42] However, the exact interaction between a peptide and a bacterium is not clearly understood. It has been proposed that initially, the peptide attaches to the target cell surface due to a general electrostatic interaction with negatively charged bacteria. This initial association is followed by a specific interaction of the peptide with a specific, yet unidentified, *L. pneumophila* membrane moiety.[43] It has also been reported that the selectivity of warnericin RK to *L. pneumophila* might be related to the fatty acid composition of the cell membrane.[43]

In our recent study, we employed a digital photocorrosion (DIP) biosensor biofunctionalized with a 16-mercaptohexadecanoic acid (MHDA) linker[54] for interfacing warnericin RK AMP, which allowed detection of *L. pneumophila* at 10^3 CFU/mL.[44] Given that a DIP biosensor is sensitive to the flow of electric charge between the biosensor and immobilized bacteria, we hypothesized that a short-linker biosensor, consisting also of a reduced number of interfaces, could exhibit a significantly enhanced sensitivity. Thus, we report here on the operation of an innovative DIP biosensor comprising cysteine-modified RK AMP (Cys-AMP) designed for rapid detection of *L. pneumophila*. A successful investigation was also carried out by demonstrating a negligible specificity of the biosensor toward *P. fluorescens*, *B. subtilis*, and *E. coli*.

2. RESULTS AND DISCUSSION

2.1. Functionalization of GaAs/AlGaAs Biosensors. The immobilization of peptides on the surface of GaAs was evaluated by FTIR analysis as presented in Figure 1 (for a detailed list of peak positions see Table S1). The FTIR absorbance spectra were obtained by subtracting from the spectrum of freshly etched GaAs (001) sample. The absorbance band at 1235 cm^{-1} was assigned to amide III, while the band at 1519 cm^{-1} could be assigned to amide II.[50,51] The absorbance at 1540 and 1655 cm^{-1} is a characteristic for C═O stretching of amide I.[52,53]

The intense bands at 2922 and 2850 cm^{-1} observed in Figure 1a are typical of CH_2 asymmetric and symmetric vibrations and are related to the thiol groups of peptides

https://dx.doi.org/10.1021/acsomega.0c04753
ACS Omega 2021, 6, 1299−1308

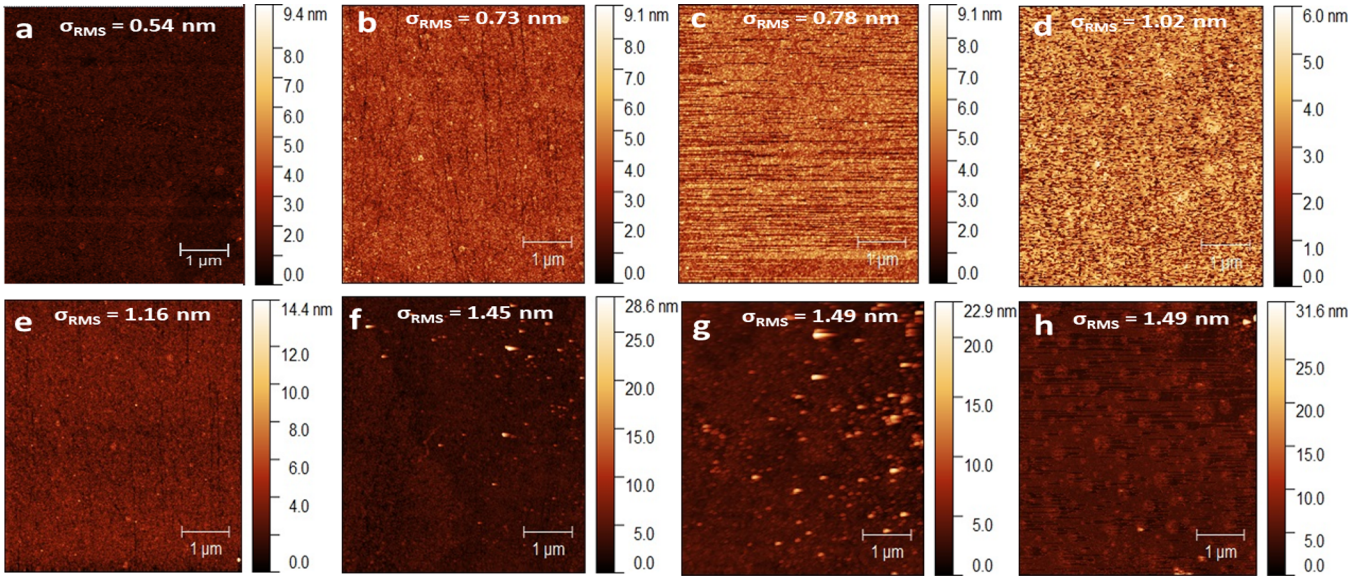

Figure 2. Representative AFM micrographs of GaAs reference surface (a), and peptide-coated GaAs at 2 (b), 5 (c), 10 (d), 25 (e), 50 (f), 75 (g), and 100 μg/mL (h).

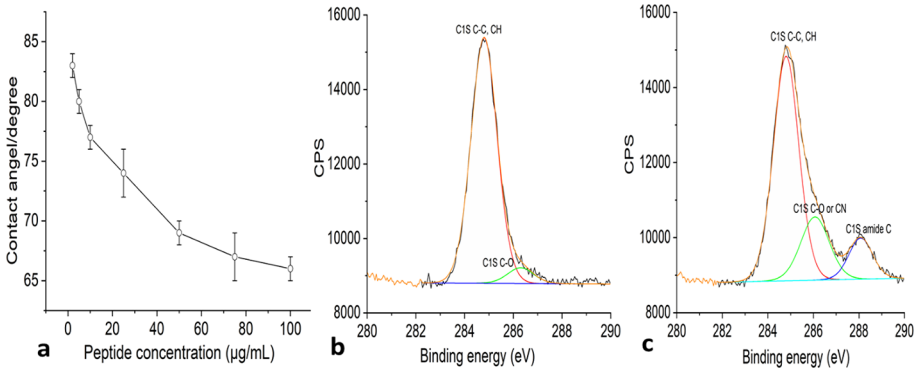

Figure 3. Water contact angle of the GaAs surface exposed to different concentrations of cysteine-modified peptides (a), and representative XPS spectra in the C 1s absorption region for the uncoated GaAs (b), and exposed to 50 μg/mL of a peptide solution (c). The error bars in (a) represent standard deviations of three repetitions.

reported in the literature.[1,32] The absorbance bands at 1653 and 1587/1734 cm^{-1} were assigned to amide I and amide II, respectively.[55,56] Similarly, the peptide immobilized at the C-terminal with a free N-terminal region shows a characteristic peak at 1653 cm^{-1}.[52,57] Furthermore, the band observed at 1734 cm^{-1} corresponds to C═O stretching of lateral chain functions and some hydrolyzed ester functions.[55,58] The intense peaks at 1653 and 1734 cm^{-1} suggest a helical conformation.[52,57,58] Furthermore, the band at 1587 cm^{-1} suggests the presence of a N−H bond for amide II,[59] while the band at 3324 cm^{-1} could be assigned to amide A.[60,61] Therefore, the amide related peaks in the FTIR spectra (1235, 1519, 1587, 1653, 1734, and 3324 cm^{-1}) confirm the successful immobilization of peptides on the surface of GaAs via the cysteine linker of peptides. It is noticeable that the peaks of a similar intensity were observed in Figure 1a for amide I, II, and III of different concentration peptides, while the amide A intensity varied with the increasing concentrations of peptides as presented in Figure 1b. The peak intensity increased with the increasing concentrations of peptides until 50 μg/mL, thereafter, the peak intensity did not correlate with higher peptide concentrations. Hence, the 50 μg/mL could be considered as the optimum peptide concentration for GaAs functionalization.

The AFM evaluation of Cys-AMP functionalized GaAs surface topography is illustrated in Figure 2, while the corresponding σ_{RMS} values are plotted in Figure S1. The micrograph in Figure 2a presents a freshly etched GaAs surface, and Figure 2b−h demonstrates the roughness of the GaAs surface functionalized with peptides of different concentrations. As shown in Figure 2a, the freshly etched GaAs surface is characterized by σ_{RMS} = 0.54 nm, which is consistent with the previously published results.[22] Following exposure to peptides at concentrations of 2, 5, 10, 25, 50, 75, and 100 μg/mL, the GaAs surface was characterized by σ_{RMS} of 0.73, 0.78, 1.02, 1.16, 1.45, 1.49, and 1.49 nm, respectively (Figure 2b−h). A comparable surface roughness is observed for GaAs exposed to 50 and 100 μg/mL of peptides, which is consistent with the saturation effect, also recorded with the FTIR measurements (Figure 1b). Clearly, the concentration of peptides at 50 μg/mL appears optimal for the functionalization of the GaAs surface.

Figure 3a illustrates the dependence of the water contact angle of the GaAs surface on the concentration of peptides employed for functionalization. The contact angle values

https://dx.doi.org/10.1021/acsomega.0c04753
ACS Omega 2021, 6, 1299−1308

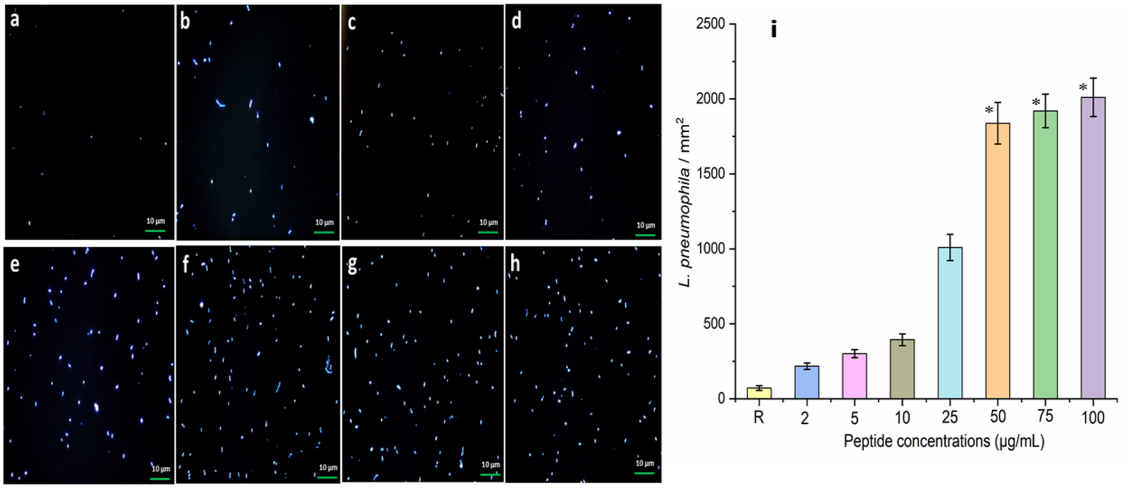

Figure 4. Representative optical micrographs of *L. pneumophila* captured on the GaAs surface using several concentrations of peptides: (a) reference, (b) 2, (c) 5, (d) 10, (e) 25, (f) 50, (g) 75, and (h) 100 μg/mL, and (i) density of captured *L. pneumophila* on the reference (R) and peptide functionalized GaAs surfaces. The asterisks indicate significantly different values compared to the reference as determined by the Student's *t* test ($n = 3$, $p < 0.05$).

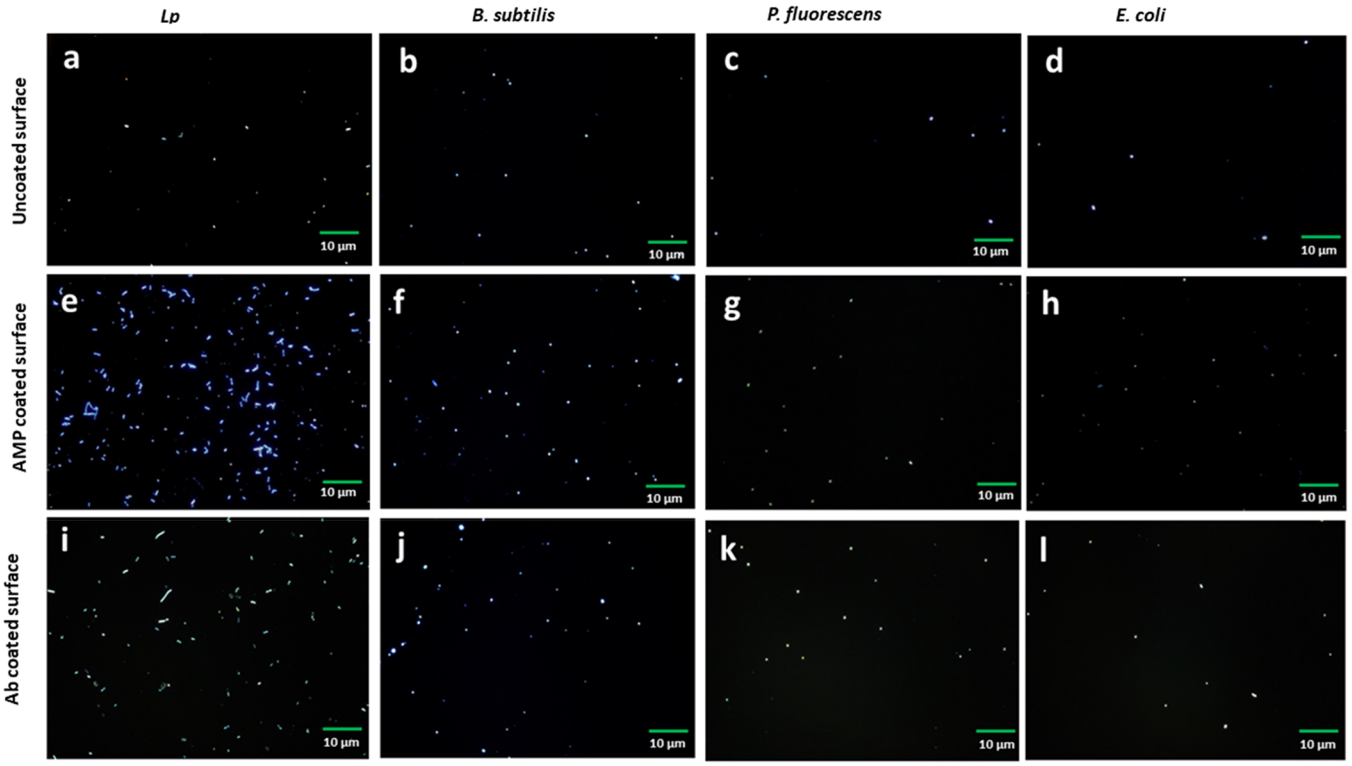

Figure 5. Representative optical micrographs of different bacteria on uncoated GaAs surface (a–d), and GaAs surfaces functionalized with AMP at 50 μg/mL (e–h) and Ab at 100 μg/mL (i–l).

decreasing from 83 to 66° were observed for surfaces functionalized with peptides at 2, 5, 10, 25, 50, 75, and 100 μg/mL. Note that the oxidized surface of GaAs is characterized by contact angles exceeding 90°.[62] The increased hydrophilicity of GaAs following the deposition of peptides is consistent with the results of Date et al.[63] who showed that the air bubble angles decreased substantially with increasing concentrations of peptides on the gold surface.

XPS data for bare and peptide functionalized (50 μg/mL) GaAs surfaces are presented in Figure 3b,c. The C 1s spectra for both functionalized and non-functionalized samples were observed at 284.8 eV, ascribed to C−H and C−C bonds.[64] The peak at 286.3 eV could be assigned to the carbon atoms of the C═O or C−N[65,66] or to the O═C—N.[64,67] The amide related peak at 288.08 eV,[67,68] observed only for the functionalized sample, confirms the presence of peptides.

2.2. Surface Coverage with Bacteria. Representative optical micrographs of the GaAs surface functionalized with different concentrations of Cys-AMP and exposed to the *L. pneumophila* suspension at 10^6 CFU/mL are shown in Figure 4a–h, while the capture efficiencies are summarized in Figure 4i. The uncoated (reference) surface of GaAs was able to

https://dx.doi.org/10.1021/acsomega.0c04753
ACS Omega 2021, 6, 1299−1308

capture ~72 bacteria/mm^2, whereas peptides at 2, 5, 10, 25, 50, 75, and 100 μg/mL yielded 217, 301, 394, 1009, 1868, 1920, and 2011 average bacteria/mm^2, respectively. The captured bacteria steadily increased with the concentration of peptide to 50 μg/mL, thereafter demonstrating a tendency toward saturation.

To evaluate the specificity of peptide toward *L. pneumophila*, a series of tests were carried out against the non-target *P. fluorescens*, *B. subtilis*, and *E. coli* bacteria at 10^6 CFU/mL with the GaAs chips functionalized with either peptides cysteine-modified warnericin RK (Cys-WRK) AMP or anti-*L. pneumophila* Ab. The representative micrographs of the biochip surfaces are shown in Figure 5, and resulting bacterial capture efficiencies are illustrated in the Figure 6. The Cys-WRK AMP functionalized biochips captured *L. pneumophila*, *B. subtilis*, *P. fluorescens*, and *E. coli*, on average, at 2018, 477, 331, and 216 bacteria/mm^2, respectively. This is compared with the ability of anti-*L. pneumophila* Ab functionalized biochips to capture the same bacteria, on average, at 742, 217, 186, and 165 bacteria/mm^2, respectively. These results clearly demonstrate that RK AMP peptide, and as expected, anti-*L. pneumophila* Ab-coated GaAs surfaces captured *L. pneumophila* more efficiently compared to other bacteria. Notably, the Cys-WRK AMP functionalized GaAs biochips captured *L. pneumophila* at least four times more efficiently than the other investigated bacteria.

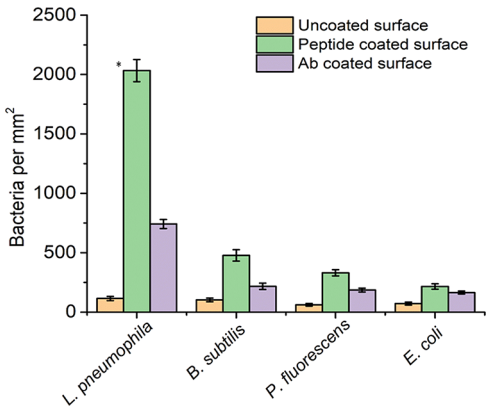

Figure 6. Summary of the results indicating that a cysteine-modified warnericin AMP biosensor captured *L. pneumophila* four times more efficiently than the other investigated bacteria. The asterisks indicate significantly different values compared to the reference ($p < 0.05$) as determined by the Students *t* test ($n = 3$).

A number of studies have evaluated binding affinity as well as interaction between peptide and bacteria on the surface of biosensor substrates. For instance, Etayash et al.[32] observed that the 24AA LeuA-conjugated gold substrate exhibited high binding specificity toward Gram-positive bacteria, while lower specificity was observed for short length peptide 14AA LeuA. In another study,[1] gold substrates functionalized with 37AA LeuA were incubated with four different bacteria (*i.e.*, *E. coli*, *Listeria innocua*, *Coronabacterium divergens*, and *Listeria monocytogenes*) and it was found that the *L. monocytogenes* demonstrated the highest binding efficiency compared to other bacteria. Recent studies have reported that *L. pneumophila* sensitivity toward warnericin could be due to the lipid composition of the bacterial membrane. Verdon et al.[43] investigated the sensitivity of *L. pneumophila* to warnericin RK and found that the presence of branched-chain fatty acids on the surface of the bacteria play a crucial role in the sensitivity of the bacteria to the peptide. *Legionella* contains unusually high amounts of phosphatidylcholines (30%), which are predominantly present in eukaryotic cells only.[69] Furthermore, phosphatidylcholine is not typically present in other bacterial cell membranes.[24,69] A number of *Legionella*-specific peptides have been reported.[24,43] Of these, only three peptides, warnericin RK being one of them, were found to be specific toward *L. pneumophila* serogroups 1, 3, 5, and 6.[24] Therefore, the results obtained here, in agreement with previous reports, suggest that the innovative warnericin RK-conjugated GaAs-based biosensor could be an attractive system for specific detection of *L. pneumophila*.

2.3. Detection of *L. pneumophila*. Detection of *L. pneumophila* was carried out with the PL effect employed for

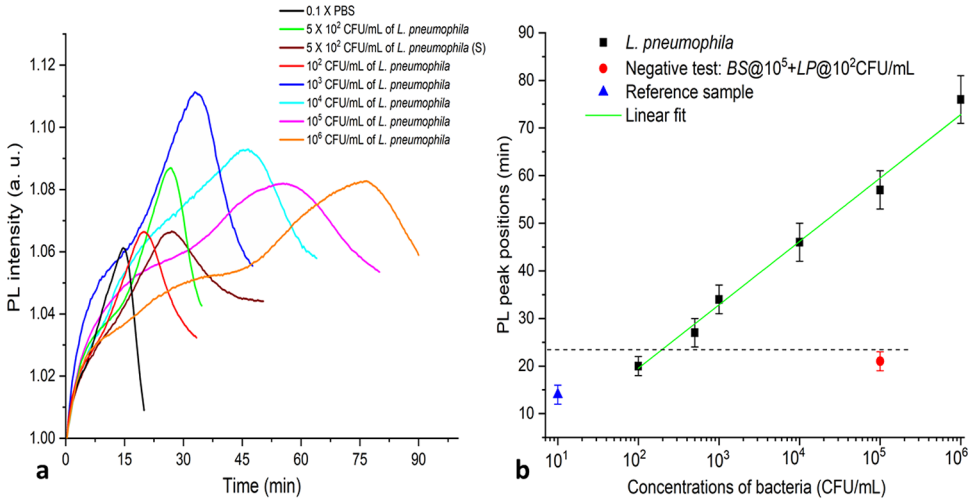

Figure 7. (a) Normalized PL intensity of AMP functionalized GaAs/AlGaAs DIP biochips (wafer D3422) exposed to different concentrations of *L. pneumophila* in 0.1 × PBS, (b) PL peak positions *vs* different concentrations of *L. pneumophila*. The PL peak positions obtained for *L. pneumophila* are statistically different compared to either 0.1× PBS (reference), 10^2 CFU/mL of *L. pneumophila*, or the negative control test for *B. subtilis* + *L. pneumophila* exposed surfaces, as determined by the Student's *t* test ($n = 3$, $p < 0.05$). The dashed line highlights the biosensing resolution of the device against peak positions of the negative test and the results obtained for *L. pneumophila* suspension at 10^2 CFU/mL.

https://dx.doi.org/10.1021/acsomega.0c04753
ACS Omega 2021, 6, 1299−1308

monitoring DIP of GaAs/AlGaAs nanoheterostructures. The PL scans of the Cys-AMP functionalized biochips exposed to different concentrations of *L. pneumophila* are shown in Figure 7. The PL maxima were observed at 15, 20, 27, 34, 46, 57, and 76 min for 0, 10^2, 5×10^2, 10^3, 10^4, 10^5, and 10^6 CFU/mL of *L. pneumophila*, respectively. The details of this experiment are summarized in Table 1. Under optimized conditions, the PL maximum at 20 min obtained for a bacterial suspension at 10^2 CFU/mL is delayed from the 15 min maximum observed for the reference sample. At the same time, the 21 min PL maximum observed for the mixed suspension of *B. subtilis* at 10^5 CFU/mL and *L. pneumophila* at 10^2 CFU/mL suggests that the limit of detection of the biosensor is at $\sim 2 \times 10^2$ CFU/mL. The delayed positions of PL maxima revealed for the growing concentrations of *L. pneumophila* are consistent with the sensitivity of DIP GaAs/AlGaAs nanoheterostructures to the presence of bacteria immobilized on the biosensor surface. In this system, the rate of photocorrosion of GaAs/AlGaAs nanoheterostructures is delayed due to the charge transfer between bacteria and the semiconductor, as suggested previously.[21,70] A mixed suspension of *B. subtilis* at 10^5 CFU/mL with *L. pneumophila* at 10^2 CFU/mL was used as a control to demonstrate the specificity of a proposed biosensor. When mixed together, the bacteria showed a PL maximum at 21 min, whereas *L. pneumophila* alone at 10^2 CFU/mL yielded a PL maximum at 20 min, which illustrates that the PL maxima were not affected in a measurable manner by the presence of non-target bacteria. We also observed that inter-experimental (different biochips) errors for determining PL maxima varied less than 13%, which indicated a relatively highly reproducible detection. Furthermore, the reproducible response of the biosensor was demonstrated for GaAs/AlGaAs chips functionalized with peptide solutions stored at room temperature for 30 days. The related PL scan, collected for *L. pneumophila* at 5×10^2 CFU/mL (sample S), revealed the PL maximum position at 27 min, which is similar to that obtained for the fresh peptide solution. A summary of several recent studies reporting on biosensing of *L. pneumophila* is provided in Table S2. Aziziyan et al.[33] detected 10^4 CFU/mL of *L. pneumophila* using an Ab functionalized GaAs/AlGaAs DIP biosensor. In their subsequent study,[21] they improved the detection limit to 10^3 CFU/mL by decorating bacteria with sodium dodecyl sulfate (SDS). However, a decoration step of bacteria with SDS increases the complexity of a detection protocol, and thus, it may not be entirely advantageous in comparison to the simple process of detecting *L. pneumophila* with a Cys-AMP-based biosensor.

Table 1. PL Maxima Obtained for the Reference (PBS) Run and Different Concentrations of *L. pneumophila* (All Experiments Repeated for at Least Three Times)

bacteria	concentrations (CFU/mL)	PL maxima (min)
PBS	0.1×	15 ± 13%
L. pneumophila	10^2	20 ± 10%
L. pneumophila	5×10^2	27 ± 11%
L. pneumophila	5×10^2(S)	27 ± 9%
L. pneumophila	10^3	34 ± 9%
L. pneumophila	10^4	46 ± 9%
L. pneumophila	10^5	57 ± 7%
L. pneumophila	10^6	76 ± 7%
B. subtilis + *L. pneumophila*	$10^5 + 10^2$	21 ± 13%

3. EXPERIMENTAL SECTION

3.1. Materials and Reagents. Undoped, double-side-polished GaAs (001) chips (Wafer WV 23084, Wafer Technology Ltd., Washington, USA) were used for measuring bacteria capture efficiency. GaAs/$Al_{0.35}Ga_{0.65}As$ nanoheterostructure wafers (Canadian Photonics Fabrication Centre, Ottawa, Ontario, Canada) were used for monitoring the DIP process of biofunctionalized chips. The details for employing GaAs/AlGaAs nanoheterostructures in DIP biochips have been reported elsewhere.[19,33] Semiconductor grade isopropanol, acetone, and OptiClear were purchased, respectively, from Fisher Scientific (Ottawa, Canada), National Diagnostics (Mississauga, Canada), and ACP (Montréal, Canada). Anhydrous ethanol was purchased from Commercial Alcohols Inc. (Brampton, Canada). Ammonium hydroxide (28% of NH_4OH) used for removing oxides from the GaAs surface was purchased from Anachemia (Richmond, Canada). Phosphate-buffered saline solution (PBS; 10×, pH 7.4) and 16-mercaptohexadecanoic acid (MHDA) thiol were purchased from Sigma-Aldrich (Oakville, Canada) and ViroStat, Inc. (Portland, ME), respectively. Anti-*L. pneumophila* polyclonal Ab were purchased from ViroStat, Inc. Green fluorescent *L. pneumophila* JR32 was obtained from the Faculty of Agricultural and Environmental Sciences, McGill University (Ste-Anne de Bellevue, Québec, Canada). *Bacillus subtilis* ATCC 60514 and *Escherichia coli* ATCC 25922 were obtained from the Department of Biology, Université de Sherbrooke (Quebec, Canada), and *Pseudomonas fluorescens* ATCC 13525 was purchased from Cedarlane (Burlington, Ontario, Canada). Cys-AMPs (GenScript, Piscataway, USA) were employed to achieve robust functionalization of GaAs/AlGaAs chips, thus, taking advantage of the strong affinity of sulfur toward Ga and As.[45]

3.2. Biofunctionalization of GaAs-Based Chip Surface. Bulk GaAs (001) chips, 2 mm × 2 mm, were used for carrying out Fourier transform infrared spectroscopy (FTIR), X-ray photoelectron spectroscopy (XPS), atomic force microscopy (AFM), and bacteria capture efficiency measurements. The samples of bulk GaAs and GaAs/AlGaAs nanoheterostructures were cleaned in ultrasonic baths of acetone, OptiClear, and isopropanol for 5 min each, and then dried with high purity nitrogen gas.[46,47] Thereafter, native oxides present on the surface of the samples were removed with 28% NH_4OH (2 min at room temperature) followed by immediate dipping of the samples in degassed ethanol and rinsing with copious amounts of degassed DI water. Different concentrations of peptide solutions (2−100 μg/mL) were prepared for functionalizing the GaAs and GaAs/AlGaAs chips. To investigate the stability of the proposed biosensor, aliquots of peptide solution (50 μg/mL) were stored at room temperature for up to 30 days. Functionalization was achieved by immersing cleaned samples in peptide solution for 1 h. The functionalized chips were sonicated in degassed DI water for 1 min and immediately rinsed with degassed DI water to remove non-immobilized peptides.

3.3. Preparation of Bacteria. *E. coli*, *P. fluorescens*, and *B. subtilis* were obtained from fresh cultures in a Luria-Bertani (LB) medium. *L. pneumophila* ssp1 were cultured in a buffered charcoal yeast extract agar (BCYE), supplemented with isopropyl thio-β-galactoside (IPTG) and L-cysteine. Subse-

https://dx.doi.org/10.1021/acsomega.0c04753
ACS Omega 2021, 6, 1299−1308

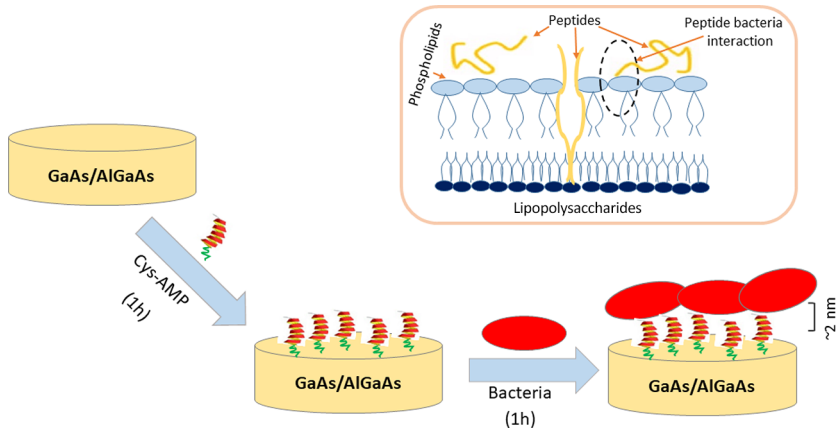

Figure 8. Cysteine-modified warnericin RK antimicrobial peptide-based architecture of the *L. pneumophila* biosensor employing GaAs/AlGaAs nanoheterostructure chips. The inset illustrates the proximity of interaction between bacterial cell membrane and peptides.

quently, after 3-day incubation, several colonies of *L. pneumophila* were transferred to 0.1× PBS, and concentration of bacteria was determined by OD_{600nm} measurement (0.1 OD 600_{nm} corresponds to 6.4×10^7 *Legionella*/mL). Serial dilutions were carried out in 0.1× PBS to achieve the test concentrations.

3.4. Biosensor Architecture. Following the removal of native oxides from the surface of GaAs/AlGaAs chips, the samples were immersed for 1 h in Cys-AMPs suspended in DI water. Subsequently, a 1 min sonication in degassed DI water was applied to remove non-immobilized peptides. However, it was found that light rinsing with DI water was sufficient to remove weakly bonded (physisorbed) peptides, which may be important for the future development of a procedure for automated biofunctionalization. The biofunctionalized chips, typically less than 60 min from their fabrication, were exposed to different suspensions of bacteria. Figure 8 illustrates the process of a biosensor fabrication. Notice that the strong interaction of warnericin RK AMP with *L. pneumophila* is expected to result in the rapid breaking of the bacterial outer membrane as illustrated by the inset in Figure 8. It is important to note that the entire detection procedure of this biosensor could be completed within ∼2 h, including the biofunctionalization step, as compared to the more than 20 h required by a biosensor employing an alkanethiol self-assembled monolayer. Furthermore, of potential importance to the operation of charge sensitive sensors (DIP, electrochemical or field-effect devices) is the remarkably short, 2 nm distance between the biochip surface and bacteria immobilized with the Cys-AMP architecture, which could affect the process of charge transfer.

In the case of anti-*L. pneumophila* Ab functionalization, the etched samples (after being treated with 28% NH_4OH) were immersed in 1 mM of MHDA thiol in 10 mL of deoxygenated ethanol for 20 h. After the thiolation, the functionalized chips were sonicated in degassed ethanol for 1 min and immediately rinsed with degassed ethanol to remove non-immobilized thiols. Thereafter, the −COOH terminals of thiolated samples were activated using 0.4 M EDC:0.1 M NHS (1:1) solution for 30 min and immediately rinsed with DI water. Then, the samples were incubated in 100 μg/mL of anti-*L. pneumophila* polyclonal Ab for 1 h. Finally, both AMP and Ab functionalized samples were incubated with heat-killed *L. pneumophila* at 10^6 CFU/mL for 1 h. The GaAs/$Al_{0.35}Ga_{0.65}As$ nanoheterostructures were used for the fabrication of 2 mm × 2 mm DIP biochips functionalized by following the aforementioned protocols. A schematic diagram of a typical sample functionalization and bacteria attachment to GaAs/AlGaAs-MHDA-AMP and GaAs/AlGaAs-MHDA-Ab functionalized biochips is presented in Figure S2.

3.5. Fourier Transform Infrared Spectroscopy Analysis. The FTIR absorption spectroscopy measurements were collected using a Bruker Optics Hyperion 2000 FTIR system. The spectra were collected with a resolution at 4 cm^{-1}, and individual spectra were averaged over 1000 scans. All FTIR data were recorded with a liquid N_2 chilled HgCdTe (mercury cadmium telluride) IR detector. A reference GaAs sample was obtained by consecutive cleanings in ultrasound baths with OptiClear, acetone, isopropanol, acetone, and ethanol (5 min each), and then etched with a 28% NH_4OH solution.

3.6. Atomic Force Microscopy Analysis. Topographic images of functionalized GaAs samples were taken with an atomic force microscope (AFM, Shimadzu Instruments, SPM-9700, Japan) operating at room temperature (∼25 ± 2 °C). The root mean square surface roughness (σ_{RMS}) was calculated based on scans collected from 5 μm × 5 μm surface areas of the investigated samples. Images were analyzed using AFM Gwyddion software (version 2.53).

3.7. X-ray Photoelectron Spectroscopy Analysis. XPS spectra were recorded with a Kratos Analytical AXIS (Ultra DLD XPS) spectrometer employing an Al Kα source (1486.6 eV) operating at 150 W. The XPS data were obtained with a 60° take-off angle with respect to the surface normal. The carbon signals were measured and fitted using Casa XPS software for both bulk GaAs and GaAs/AlGaAs biochip samples. The binding energy reference to the adventitious C 1s peak at 284.8 eV positioned the As $3d_{5/2}$ peak at 40.8 eV, which was subsequently used as a nominal calibration.

3.8. Contact Angle Measurements. The water hydrophilicity of the peptide functionalized GaAs surface was determined at room temperature using commercial static water contact angle measurement equipment (KRÜSS DSA30). The GaAs surface was exposed to a 10 μL droplet of Milli-Q water, and after 5 s, the contact angle of the GaAs-water interface was calculated.

3.9. Optical Microscopy Analysis. Optical microscopy (Nikon Instruments, Inc.) was used to determine the density of immobilized bacteria on the biochip surface. The images were taken at 200× magnification in three different regions of each sample surface. All experiments were repeated at least

https://dx.doi.org/10.1021/acsomega.0c04753
ACS Omega 2021, 6, 1299−1308

three times. The bacteria surface coverage was calculated using ImageJ software.[48]

3.10. Photoluminescence Measurements. The detection of bacteria was carried out at room temperature with a DIP GaAs/AlGaAs biosensor whose PL was measured with a quantum semiconductor photonic biosensing (QSPB) reader described elsewhere.[33,49] Reference measurements and bacteria-coated biochips were irradiated with 5 s pulses delivering 17 mW/cm^2 each, in every 20 s period, using a light emitting diode (LED) operating at a wavelength of 660 nm. The PL signal and images of the biochips collected *in situ* were recorded with a charge-coupled device (CCD) camera. Experiments were carried out in a 0.1× PBS solution, and runs without bacteria were used to obtain the reference signal. All experiments were repeated at least three times.

4. CONCLUSIONS

This study has demonstrated the innovative concept of a cysteine-modified warnericin RK antimicrobial peptide (Cys-AMP) architecture for construction of a biosensor for rapid detection of *L. pneumophila* in an aqueous environment. The biosensing architecture was employed for functionalization of GaAs/AlGaAs nanoheterostructure biosensors operating on the principle of a digital photocorrosion. The role of peptide concentration on the efficiency of capturing *L. pneumophila* was investigated with FTIR, AFM, XPS, and water contact angle measurements. The absorbance band peaks related to peptide, observed at 1653 cm^{-1} (amide I), 1734 cm^{-1}/1538 cm^{-1} (amide II) and 3324 cm^{-1} (amide A), confirmed the chemisorption of peptide on the GaAs surface. Our results showed that 50 μg/mL of Cys-AMP was the optimum concentration as determined by maximum capture of *L. pneumophila* visualized with optical microscopy. The detection sensitivity of the developed biosensor was investigated in the range of 10^2 to 10^6 CFU/mL of *L. pneumophila*, with the limit of detection estimated at 2×10^2 CFU/mL. Thus, the investigated GaAs/AlGaAs nanoheterostructure DIP biosensors demonstrate functionality, which is attractive for the rapid and direct detection of *L. pneumophila* present in a water environment at a relatively low concentration. The specificity of the biosensor was rated against *P. fluorescens*, *B. subtilis*, and *E. coli* abundantly found in samples of the environmental water. The Cys-AMP functionalized GaAs biochips showed a capture efficiency of over four times greater for *L. pneumophila* compared to the other investigated bacteria. The important consequence of the proposed Cys-AMP biosensing architecture is that it requires a relatively short time for completion, which may be found attractive for the operation of other biosensors of *L. pneumophila* compatible with the thiolation procedure. Furthermore, the short length of the employed ligand could potentially result in an enhanced charge transfer between bacteria and the biochip surface, thus leading to an enhanced performance of charge sensing biosensors.

ASSOCIATED CONTENT

Supporting Information

The Supporting Information is available free of charge at https://pubs.acs.org/doi/10.1021/acsomega.0c04753.

Schematic representation of antibody and AMP-based GaAs biofunctionalization, the root-mean-square roughness values of the GaAs functionalization with peptide, FTIR absorbance bands corresponding to the assigned functional groups, examples of immunosensor-based detection of *L. pneumophila* (PDF)

AUTHOR INFORMATION

Corresponding Author

Jan J. Dubowski − *Interdisciplinary Institute for Technological Innovation (3IT), CNRS UMI-3463, Laboratory for Quantum Semiconductors and Photon-based BioNanotechnology, Department of Electrical and Computer Engineering, Université de Sherbrooke, Sherbrooke, Québec J1K 0A5, Canada;* orcid.org/0000-0003-0022-527X; Phone: +1 819 821 8000 x62528; Email: jan.j.dubowski@usherbrooke.ca.; Fax: +1 819 821 7937

Authors

M. Amirul Islam − *Interdisciplinary Institute for Technological Innovation (3IT), CNRS UMI-3463, Laboratory for Quantum Semiconductors and Photon-based BioNanotechnology, Department of Electrical and Computer Engineering, Université de Sherbrooke, Sherbrooke, Québec J1K 0A5, Canada*

Walid M. Hassen − *Interdisciplinary Institute for Technological Innovation (3IT), CNRS UMI-3463, Laboratory for Quantum Semiconductors and Photon-based BioNanotechnology, Department of Electrical and Computer Engineering, Université de Sherbrooke, Sherbrooke, Québec J1K 0A5, Canada*

Azam F. Tayabali − *Environmental Health Science Research Bureau, Healthy Environments and Consumer Safety Branch, Health Canada, Ottawa, Ontario K1A 0K9, Canada;* orcid.org/0000-0002-6037-5619

Complete contact information is available at: https://pubs.acs.org/10.1021/acsomega.0c04753

Notes

The authors declare no competing financial interest.

ACKNOWLEDGMENTS

This project was supported by the Natural Sciences and Engineering Research Council of Canada (NSERC) Strategic Partnership grant no. SPG-2016-494057, and the NSERC Discovery Grant RGPIN-2015-04448. The fabrication of GaAs/AlGaAs wafers was subsidized by CMC Microsystems (Kingston, Canada). M.A.I. acknowledges the B2X scholarship from the Fonds de Recherche sur la Nature et les Technologies du Québec (FRQNT). The authors are indebted to Prof. E.H. Frost and Dr. K. Moumanis for helpful discussions.

REFERENCES

(1) Etayash, H.; Norman, L.; Thundat, T.; Stiles, M.; Kaur, K. Surface-conjugated antimicrobial peptide leucocin a displays high binding to pathogenic gram-positive bacteria. *ACS Appl. Mater. Interfaces* **2014**, *6*, 1131−1138.

(2) Ashbolt, N. J. Microbial contamination of drinking water and disease outcomes in developing regions. *Toxicology* **2004**, *198*, 229−238.

(3) Teles, F. S. R. R.; de Tavora Tavira, L. A. P.; da Fonseca, L. J. P. Biosensors as rapid diagnostic tests for tropical diseases. *Crit. Rev. Clin. Lab. Sci.* **2010**, *47*, 139−169.

(4) Hameed, S.; Xie, L.; Ying, Y. Conventional and emerging detection techniques for pathogenic bacteria in food science: A review. *Trends Food Sci. Technol.* **2018**, *81*, 61−73.

(5) Jayan, H.; Pu, H.; Sun, D.-W. Recent development in rapid detection techniques for microorganism activities in food matrices

using bio-recognition: A review. *Trends Food Sci. Technol.* **2020**, 233−246.
(6) Keserue, H. A.; Baumgartner, A.; Felleisen, R.; Egli, T. Rapid detection of total and viable L egionella pneumophila in tap water by immunomagnetic separation, double fluorescent staining and flow cytometry. *Microb. Biotechnol.* **2012**, *5*, 753−763.
(7) Mothershed, E. A.; Whitney, A. M. Nucleic acid-based methods for the detection of bacterial pathogens: present and future considerations for the clinical laboratory. *Clin. Chim. Acta* **2006**, *363*, 206−220.
(8) Jeverica, S.; Nagy, E.; Mueller-Premru, M.; Papst, L. Sample preparation method influences direct identification of anaerobic bacteria from positive blood culture bottles using MALDI-TOF MS. *Anaerobe* **2018**, *54*, 231−235.
(9) Singhal, N.; Kumar, M.; Kanaujia, P. K.; Virdi, J. S. MALDI-TOF mass spectrometry: an emerging technology for microbial identification and diagnosis. *Front. Microbiol.* **2015**, *6*, 791.
(10) Buchan, B. W.; Ledeboer, N. A. Emerging technologies for the clinical microbiology laboratory. *Clin. Microbiol. Rev.* **2014**, *27*, 783−822.
(11) Hoyos-Nogués, M.; Gil, F. J.; Mas-Moruno, C. Antimicrobial peptides: powerful biorecognition elements to detect bacteria in biosensing technologies. *Molecules* **2018**, *23*, 1683.
(12) Yoo, S. M.; Lee, S. Y. Optical biosensors for the detection of pathogenic microorganisms. *Trends Biotechnol.* **2016**, *34*, 7−25.
(13) Meneghello, A.; Sonato, A.; Ruffato, G.; Zacco, G.; Romanato, F. A novel high sensitive surface plasmon resonance Legionella pneumophila sensing platform. *Sens. Actuators, B* **2017**, *250*, 351−355.
(14) Miranda-Castro, R.; de-los-Santos-Álvarez, P.; Lobo-Castañón, M. J.; Miranda-Ordieres, A. J.; Tuñón-Blanco, P. Hairpin-DNA probe for enzyme-amplified electrochemical detection of Legionella pneumophila. *Anal. Chem.* **2007**, *79*, 4050−4055.
(15) Gupta, S.; Kakkar, V., Development of Environmental Biosensors for Detection, Monitoring, and Assessment. In *Nanomat. Environ. Biotechnol.* Springer: 2020; pp. 107−125.
(16) Laribi, A.; Allegra, S.; Souiri, M.; Mzoughi, R.; Othmane, A.; Girardot, F. Legionella pneumophila sg1-sensing signal enhancement using a novel electrochemical immunosensor in dynamic detection mode. *Talanta* **2020**, 120904.
(17) Mobed, A.; Hasanzadeh, M.; Hassanpour, S.; Saadati, A.; Agazadeh, M.; Mokhtarzadeh, A. An innovative nucleic acid based biosensor toward detection of Legionella pneumophila using DNA immobilization and hybridization: A novel genosensor. *Microchem. J.* **2019**, *148*, 708−716.
(18) Duplan, V.; Frost, E.; Dubowski, J. J. A photoluminescence-based quantum semiconductor biosensor for rapid in situ detection of Escherichia coli. *Sens. Actuators, B* **2011**, *160*, 46−51.
(19) Nazemi, E.; Aithal, S.; Hassen, W. M.; Frost, E. H.; Dubowski, J. J. GaAs/AlGaAs heterostructure based photonic biosensor for rapid detection of Escherichia coli in phosphate buffered saline solution. *Sens. Actuators, B* **2015**, *207*, 556−562.
(20) Nazemi, E.; Hassen, W. M.; Frost, E. H.; Dubowski, J. J. Growth of Escherichia coli on the GaAs (001) surface. *Talanta* **2018**, *178*, 69−77.
(21) Aziziyan, M. R.; Hassen, W. M.; Sharma, H.; Sani, E. S.; Annabi, N.; Frost, E. H.; Dubowski, J. J. Sodium dodecyl sulfate decorated Legionella pneumophila for enhanced detection with a GaAs/AlGaAs nanoheterostructure biosensor. *Sens. Actuators, B* **2020**, *304*, 127007.
(22) Aziziyan, M. R.; Sharma, H.; Dubowski, J. J. Photo-Atomic Layer Etching of GaAs/AlGaAs Nanoheterostructures. *ACS Appl. Mater. Interfaces* **2019**, *11*, 17968−17978.
(23) Guyard, C.; Low, D. E. Legionella infections and travel associated legionellosis. *Travel Med. Infect. Dis.* **2011**, *9*, 176−186.
(24) Berjeaud, J.-M.; Chevalier, S.; Schlusselhuber, M.; Portier, E.; Loiseau, C.; Aucher, W.; Lesouhaitier, O.; Verdon, J. Legionella pneumophila: the paradox of a highly sensitive opportunistic waterborne pathogen able to persist in the environment. *Front. Microbiol.* **2016**, *7*, 486.
(25) Marchand, A.; Verdon, J.; Lacombe, C.; Crapart, S.; Héchard, Y.; Berjeaud, J. M. Anti-Legionella activity of staphylococcal hemolytic peptides. *Peptides* **2011**, *32*, 845−851.
(26) Verdon, J.; Berjeaud, J.-M.; Lacombe, C.; Héchard, Y. Characterization of anti-Legionella activity of warnericin RK and delta-lysin I from Staphylococcus warneri. *Peptides* **2008**, *29*, 978−984.
(27) Dusserre, E.; Ginevra, C.; Hallier-Soulier, S.; Vandenesch, F.; Festoc, G.; Etienne, J.; Jarraud, S.; Molmeret, M. A PCR-based method for monitoring Legionella pneumophila in water samples detects viable but noncultivable legionellae that can recover their cultivability. *Appl. Environ. Microbiol.* **2008**, *74*, 4817−4824.
(28) Ballard, A. L.; Fry, N. K.; Chan, L.; Surman, S. B.; Lee, J. V.; Harrison, T. G.; Towner, K. J. Detection of Legionella pneumophilausing a real-time PCR hybridization assay. *J. Clin. Microbiol.* **2000**, *38*, 4215−4218.
(29) Ramanavičius, A.; Ramanavičienė, A.; Malinauskas, A. Electrochemical sensors based on conducting polymer—polypyrrole. *Electrochim. Acta* **2006**, *51*, 6025−6037.
(30) Elakkiya, E.; Matheswaran, M. Comparison of anodic metabolisms in bioelectricity production during treatment of dairy wastewater in Microbial Fuel Cell. *Bioresour. Technol.* **2013**, *136*, 407−412.
(31) Mannoor, M. S.; Zhang, S.; Link, A. J.; McAlpine, M. C. Electrical detection of pathogenic bacteria via immobilized antimicrobial peptides. *Proc. Natl. Acad. Sci.* **2010**, *107*, 19207−19212.
(32) Etayash, H.; Norman, L.; Thundat, T.; Kaur, K. Peptide-bacteria interactions using engineered surface-immobilized peptides from class IIa bacteriocins. *Langmuir* **2013**, *29*, 4048−4056.
(33) Aziziyan, M. R.; Hassen, W. M.; Morris, D.; Frost, E. H.; Dubowski, J. J. Photonic biosensor based on photocorrosion of GaAs/AlGaAs quantum heterostructures for detection of Legionella pneumophila. *Biointerphases* **2016**, *11*, No. 019301.
(34) de Miranda, J. L.; Oliveira, M. D. L.; Oliveira, I. S.; Frias, I. A. M.; Franco, O. L.; Andrade, C. A. S. A simple nanostructured biosensor based on clavanin A antimicrobial peptide for gram-negative bacteria detection. *Biochem. Eng. J.* **2017**, *124*, 108−114.
(35) Dong, Z.-M.; Zhao, G.-C. Label-free detection of pathogenic bacteria via immobilized antimicrobial peptides. *Talanta* **2015**, *137*, 55−61.
(36) Friedrich, C.; Scott, M. G.; Karunaratne, N.; Yan, H.; Hancock, R. E. Salt-resistant alpha-helical cationic antimicrobial peptides. *Antimicrob. Agents Chemother.* **1999**, *43*, 1542−1548.
(37) Rydlo, T.; Rotem, S.; Mor, A. Antibacterial properties of dermaseptin S4 derivatives under extreme incubation conditions. *Antimicrob. Agents Chemother.* **2006**, *50*, 490−497.
(38) Kulagina, N. V.; Lassman, M. E.; Ligler, F. S.; Taitt, C. R. Antimicrobial peptides for detection of bacteria in biosensor assays. *Anal. Chem.* **2005**, *77*, 6504−6508.
(39) Andrade, C. A. S.; Nascimento, J. M.; Oliveira, I. S.; de Oliveira, C. V. J.; de Melo, C. P.; Franco, O. L.; Oliveira, M. D. L. Nanostructured sensor based on carbon nanotubes and clavanin A for bacterial detection. *Colloids Surf., B* **2015**, *135*, 833−839.
(40) Kulagina, N. V.; Shaffer, K. M.; Anderson, G. P.; Ligler, F. S.; Taitt, C. R. Antimicrobial peptide-based array for Escherichia coli and Salmonella screening. *Anal. Chim. Acta* **2006**, *575*, 9−15.
(41) Hossein-Nejad-Ariani, H.; Kim, T.; Kaur, K. Peptide-based biosensor utilizing fluorescent gold nanoclusters for detection of Listeria monocytogenes. *ACS Appl. Nano Mater.* **2018**, 3389.
(42) Marchand, A.; Augenstreich, J.; Loiseau, C.; Verdon, J.; Lecomte, S.; Berjeaud, J.-M. Effect of amino acid substitution in the staphylococcal peptides warnericin RK and PSMα on their anti-Legionella and hemolytic activities. *Mol. Cell. Biochem.* **2015**, *405*, 159−167.
(43) Verdon, J.; Labanowski, J.; Sahr, T.; Ferreira, T.; Lacombe, C.; Buchrieser, C.; Berjeaud, J.-M.; Héchard, Y. Fatty acid composition modulates sensitivity of Legionella pneumophila to warnericin RK, an antimicrobial peptide. *Biochim. Biophys. Acta, Biomembr.* **2011**, *1808*, 1146−1153.

https://dx.doi.org/10.1021/acsomega.0c04753
ACS Omega 2021, 6, 1299−1308

(44) Islam, M. A.; Hassen, W. M.; Tayabali, A. F.; Dubowski, J. J. Antimicrobial warnericin RK peptide functionalized GaAs/AlGaAs biosensor for highly sensitive and selective detection of Legionella pneumophila. *Biochem. Eng. J.* **2020**, *154*, 107435.
(45) Voznyy, O.; Dubowski, J. J. c (4× 2) structures of alkanethiol monolayers on Au (111) compatible with the constraint of dense packing. *Langmuir* **2009**, *25*, 7353−7358.
(46) Lacour, V.; Elie-Caille, C.; Leblois, T.; Dubowski, J. J. Regeneration of a thiolated and antibody functionalized GaAs (001) surface using wet chemical processes. *Biointerphases* **2016**, *11*, No. 019302.
(47) Sharma, H.; Moumanis, K.; Dubowski, J. J. pH-Dependent Photocorrosion of GaAs/AlGaAs Quantum Well Microstructures. *J. Phys. Chem. C* **2016**, *120*, 26129−26137.
(48) Grishagin, I. V. Automatic cell counting with ImageJ. *Anal. Biochem.* **2015**, *473*, 63−65.
(49) Aithal, S.; Liu, N.; Dubowski, J. J. Photocorrosion metrology of photoluminescence emitting GaAs/AlGaAs heterostructures. *J. Phys. D: Appl. Phys.* **2017**, *50*, No. 035106.
(50) de Campos Vidal, B.; Mello, M. L. S. FT-IR microspectroscopy of rat ear cartilage. *PLoS One* **2016**, *11*, No. e0151989.
(51) Munje, R. D.; Muthukumar, S.; Jagannath, B.; Prasad, S. A new paradigm in sweat based wearable diagnostics biosensors using Room Temperature Ionic Liquids (RTILs). *Sci. Rep.* **2017**, *7*, 1950.
(52) Ami, D.; Posteri, R.; Mereghetti, P.; Porro, D.; Doglia, S. M.; Branduardi, P. Fourier transform infrared spectroscopy as a method to study lipid accumulation in oleaginous yeasts. *Biotechnol. biofuels* **2014**, *7*, 12.
(53) Akrami, M.; Balalaie, S.; Hosseinkhani, S.; Alipour, M.; Salehi, F.; Bahador, A.; Haririan, I. Tuning the anticancer activity of a novel pro-apoptotic peptide using gold nanoparticle platforms. *Sci. Rep.* **2016**, *6*, 31030.
(54) Huang, X.; Liu, N.; Moumanis, K.; Dubowski, J. J. Water-Mediated Self-Assembly of 16-Mercaptohexadecanoic Acid on GaAs (001). *J. Phys. Chem. C* **2013**, *117*, 15090−15097.
(55) Humblot, V.; Yala, J.-F.; Thebault, P.; Boukerma, K.; Héquet, A.; Berjeaud, J.-M.; Pradier, C.-M. The antibacterial activity of Magainin I immobilized onto mixed thiols Self-Assembled Monolayers. *Biomaterials* **2009**, *30*, 3503−3512.
(56) Forsting, T.; Gottschalk, H. C.; Hartwig, B.; Mons, M.; Suhm, M. A. Correcting the record: the dimers and trimers of trans-N-methylacetamide. *Phys. Chem. Chem. Phys.* **2017**, *19*, 10727−10737.
(57) Barbosa, M.; Vale, N.; Costa, F. M. T. A.; Martins, M. C. L.; Gomes, P. Tethering antimicrobial peptides onto chitosan: Optimization of azide-alkyne "click" reaction conditions. *Carbohydr. Polym.* **2017**, *165*, 384−393.
(58) Doiron, K.; Beaulieu, L.; St-Louis, R.; Lemarchand, K. Reduction of bacterial biofilm formation using marine natural antimicrobial peptides. *Colloids Surf., B* **2018**, *167*, 524−530.
(59) Rai, A.; Pinto, S.; Evangelista, M. B.; Gil, H.; Kallip, S.; Ferreira, M. G.; Ferreira, L. High-density antimicrobial peptide coating with broad activity and low cytotoxicity against human cells. *Acta Biomater.* **2016**, *33*, 64−77.
(60) Jeevithan, E.; Bao, B.; Bu, Y.; Zhou, Y.; Zhao, Q.; Wu, W. Type II collagen and gelatin from silvertip shark (Carcharhinus albimarginatus) cartilage: Isolation, purification, physicochemical and antioxidant properties. *Mar. Drugs* **2014**, *12*, 3852−3873.
(61) Dinesh, B.; Squillaci, M. A.; Ménard-Moyon, C.; Samorì, P.; Bianco, A. Self-assembly of diphenylalanine backbone homologues and their combination with functionalized carbon nanotubes. *Nanoscale* **2015**, *7*, 15873−15879.
(62) Gocalinska, A.; Gradkowski, K.; Dimastrodonato, V.; Mereni, L. O.; Juska, G.; Huyet, G.; Pelucchi, E. Wettability and "petal effect" of GaAs native oxides. *J. Appl. Phys.* **2011**, *110*, No. 034319.
(63) Date, T.; Sawada, T.; Serizawa, T. Self-assembled peptides on polymer surfaces: towards morphology-dependent surface functionalization. *Soft Matter* **2013**, *9*, 3469−3472.
(64) Wang, J.; Tao, K.; Yang, Y.; Zhang, L.; Wang, D.; Cao, M.; Sun, Y.; Xia, D. Short peptide mediated self-assembly of platinum nanocrystals with selective spreading property. *RSC Adv.* **2016**, *6*, 58099−58105.
(65) Oger, P.-C.; Piesse, C.; Ladram, A.; Humblot, V. Engineering of antimicrobial surfaces by using temporin analogs to tune the biocidal/antiadhesive effect. *Molecules* **2019**, *24*, 814.
(66) Fears, K. P.; Petrovykh, D. Y.; Clark, T. D. Evaluating protocols and analytical methods for peptide adsorption experiments. *Biointerphases* **2013**, *8*, 20.
(67) Soylemez, S.; Demir, B.; Eyrilmez, G. O.; Kesici, S.; Saylam, A.; Odaci Demirkol, D.; Özçubukçu, S.; Timur, S.; Toppare, L. Comparative cell adhesion properties of cysteine extended peptide architectures. *RSC Adv.* **2016**, *6*, 2695−2702.
(68) Corrales-Ureña, Y. R.; Souza-Schiaber, Z.; Lisboa-Filho, P. N.; Marquenet, F.; Noeske, P.-L. M.; Gütjen, L.; Rischka, K. Functionalization of hydrophobic surfaces with antimicrobial peptides immobilized on a bio-interfactant layer. *RSC Adv.* **2020**, *10*, 376−386.
(69) Conover, G. M.; Martinez-Morales, F.; Heidtman, M. I.; Luo, Z. Q.; Tang, M.; Chen, C.; Geiger, O.; Isberg, R. R. Phosphatidylcholine synthesis is required for optimal function of Legionella pneumophila virulence determinants. *Cell. Microbiol.* **2008**, *10*, 514−528.
(70) Nazemi, E.; Hassen, W. M.; Frost, E. H.; Dubowski, J. J. Monitoring growth and antibiotic susceptibility of Escherichia coli with photoluminescence of GaAs/AlGaAs quantum well microstructures. *Biosens. Bioelectron.* **2017**, *93*, 234−240.

https://dx.doi.org/10.1021/acsomega.0c04753
ACS Omega 2021, 6, 1299−1308